

K/π Fluctuations at Relativistic Energies

B. I. Abelev,⁸ M. M. Aggarwal,³⁰ Z. Ahammed,⁴⁷ B. D. Anderson,¹⁸ D. Arkhipkin,¹² G. S. Averichev,¹¹ J. Balewski,²² O. Barannikova,⁸ L. S. Barnby,² J. Baudot,¹⁶ S. Baumgart,⁵² D. R. Beavis,³ R. Bellwied,⁵⁰ F. Benedosso,²⁷ M. J. Betancourt,²² R. R. Betts,⁸ A. Bhasin,¹⁷ A. K. Bhati,³⁰ H. Bichsel,⁴⁹ J. Bielcik,¹⁰ J. Bielcikova,¹⁰ B. Biritz,⁶ L. C. Bland,³ M. Bombara,² B. E. Bonner,³⁶ M. Botje,²⁷ J. Bouchet,¹⁸ E. Braidot,²⁷ A. V. Brandin,²⁵ E. Bruna,⁵² S. Bueltmann,²⁹ T. P. Burton,² M. Bystersky,¹⁰ X. Z. Cai,⁴⁰ H. Caines,⁵² M. Calderón de la Barca Sánchez,⁵ O. Catu,⁵² D. Cebra,⁵ R. Cendejas,⁶ M. C. Cervantes,⁴² Z. Chajecki,²⁸ P. Chaloupka,¹⁰ S. Chattopadhyay,⁴⁷ H. F. Chen,³⁸ J. H. Chen,¹⁸ J. Y. Chen,⁵¹ J. Cheng,⁴⁴ M. Cherney,⁹ A. Chikanian,⁵² K. E. Choi,³⁴ W. Christie,³ R. F. Clarke,⁴² M. J. M. Codrington,⁴² R. Corliss,²² T. M. Cormier,⁵⁰ M. R. Cosentino,³⁷ J. G. Cramer,⁴⁹ H. J. Crawford,⁴ D. Das,⁵ S. Das,⁴⁷ S. Dash,¹³ M. Daugherty,⁴³ L. C. De Silva,⁵⁰ T. G. Dedovich,¹¹ M. DePhillips,³ A. A. Derevschikov,³² R. Derradi de Souza,⁷ L. Didenko,³ P. Djawotho,⁴² S. M. Dogra,¹⁷ X. Dong,²¹ J. L. Drachenberg,⁴² J. E. Draper,⁵ J. C. Dunlop,³ M. R. Dutta Mazumdar,⁴⁷ W. R. Edwards,²¹ L. G. Efimov,¹¹ E. Elhalhuli,² M. Elnimr,⁵⁰ V. Emelianov,²⁵ J. Engelage,⁴ G. Eppley,³⁶ B. Erasmus,⁴¹ M. Estienne,⁴¹ L. Eun,³¹ P. Fachini,³ R. Fatemi,¹⁹ J. Fedorisin,¹¹ A. Feng,⁵¹ P. Filip,¹² E. Finch,⁵² V. Fine,³ Y. Fisyak,³ C. A. Gagliardi,⁴² L. Gaillard,² D. R. Gangadharan,⁶ M. S. Ganti,⁴⁷ E. J. Garcia-Solis,⁸ A. Geromitsos,⁴¹ F. Geurts,³⁶ V. Ghazikhanian,⁶ P. Ghosh,⁴⁷ Y. N. Gorbunov,⁹ A. Gordon,³ O. Grebenyuk,²¹ D. Grosnick,⁴⁶ B. Grube,³⁴ S. M. Guertin,⁶ K. S. F. F. Guimaraes,³⁷ A. Gupta,¹⁷ N. Gupta,¹⁷ W. Guryn,³ B. Haag,⁵ T. J. Hallman,³ A. Hamed,⁴² J. W. Harris,⁵² W. He,¹⁵ M. Heinz,⁵² S. Heppelmann,³¹ B. Hippolyte,¹⁶ A. Hirsch,³³ E. Hjort,²¹ A. M. Hoffman,²² G. W. Hoffmann,⁴³ D. J. Hofman,⁸ R. S. Hollis,⁸ H. Z. Huang,⁶ T. J. Humanic,²⁸ L. Huo,⁴² G. Igo,⁶ A. Iordanova,⁸ P. Jacobs,²¹ W. W. Jacobs,¹⁵ P. Jakl,¹⁰ C. Jena,¹³ F. Jin,⁴⁰ C. L. Jones,²² P. G. Jones,² J. Joseph,¹⁸ E. G. Judd,⁴ S. Kabana,⁴¹ K. Kajimoto,⁴³ K. Kang,⁴⁴ J. Kapitan,¹⁰ D. Keane,¹⁸ A. Kechechyan,¹¹ D. Kettler,⁴⁹ V. Yu. Khodyrev,³² D. P. Kikola,²¹ J. Kiryluk,²¹ A. Kisiel,²⁸ S. R. Klein,²¹ A. G. Knospe,⁵² A. Kocoloski,²² D. D. Koetke,⁴⁶ M. Kopytine,¹⁸ W. Korsch,¹⁹ L. Kotchenda,²⁵ V. Kouchpil,¹⁰ P. Kravtsov,²⁵ V. I. Kravtsov,³² K. Krueger,¹ M. Krus,¹⁰ C. Kuhn,¹⁶ L. Kumar,³⁰ P. Kurnadi,⁶ M. A. C. Lamont,³ J. M. Landgraf,³ S. LaPointe,⁵⁰ J. Lauret,³ A. Lebedev,³ R. Lednicki,¹² C.-H. Lee,³⁴ J. H. Lee,³ W. Leight,²² M. J. LeVine,³ C. Li,³⁸ N. Li,⁵¹ Y. Li,⁴⁴ G. Lin,⁵² S. J. Lindenbaum,²⁶ M. A. Lisa,²⁸ F. Liu,⁵¹ J. Liu,³⁶ L. Liu,⁵¹ T. Ljubicic,³ W. J. Llope,³⁶ R. S. Longacre,³ W. A. Love,³ Y. Lu,³⁸ T. Ludlam,³ G. L. Ma,⁴⁰ Y. G. Ma,⁴⁰ D. P. Mahapatra,¹³ R. Majka,⁵² O. I. Mall,⁵ L. K. Mangotra,¹⁷ R. Manweiler,⁴⁶ S. Margetis,¹⁸ C. Markert,⁴³ H. S. Matis,²¹ Yu. A. Matulenko,³² D. McDonald,³⁶ T. S. McShane,⁹ A. Meschanin,³² R. Milner,²² N. G. Minaev,³² S. Mioduszewski,⁴² A. Mischke,²⁷ B. Mohanty,⁴⁷ D. A. Morozov,³² M. G. Munhoz,³⁷ B. K. Nandi,¹⁴ C. Nattrass,⁵² T. K. Nayak,⁴⁷ J. M. Nelson,² P. K. Netrakanti,³³ M. J. Ng,⁴ L. V. Nogach,³² S. B. Nurushev,³² G. Odyniec,²¹ A. Ogawa,³ H. Okada,³ V. Okorokov,²⁵ D. Olson,²¹ M. Pachr,¹⁰ B. S. Page,¹⁵ S. K. Pal,⁴⁷ Y. Pandit,¹⁸ Y. Panebratsev,¹¹ T. Pawlak,⁴⁸ T. Peitzmann,²⁷ V. Perevoztchikov,³ C. Perkins,⁴ W. Peryt,⁴⁸ S. C. Phatak,¹³ P. Pile,³ M. Planinic,⁵³ J. Pluta,⁴⁸ D. Plyku,²⁹ N. Poljak,⁵³ A. M. Poskanzer,²¹ B. V. K. S. Potukuchi,¹⁷ D. Prindle,⁴⁹ C. Pruneau,⁵⁰ N. K. Pruthi,³⁰ P. R. Pujahari,¹⁴ J. Putschke,⁵² R. Raniwala,³⁵ S. Raniwala,³⁵ R. Redwine,²² R. Reed,⁵ A. Ridiger,²⁵ H. G. Ritter,²¹ J. B. Roberts,³⁶ O. V. Rogachevskiy,¹¹ J. L. Romero,⁵ A. Rose,²¹ C. Roy,⁴¹ L. Ruan,³ M. J. Russcher,²⁷ R. Sahoo,⁴¹ I. Sakrejda,²¹ T. Sakuma,²² S. Salur,²¹ J. Sandweiss,⁵² M. Sarsour,⁴² J. Schambach,⁴³ R. P. Scharenberg,³³ N. Schmitz,²³ J. Seger,⁹ I. Selyuzhenkov,¹⁵ P. Seyboth,²³ A. Shabetai,¹⁶ E. Shahaliev,¹¹ M. Shao,³⁸ M. Sharma,⁵⁰ S. S. Shi,⁵¹ X.-H. Shi,⁴⁰ E. P. Sichtermann,²¹ F. Simon,²³ R. N. Singaraju,⁴⁷ M. J. Skoby,³³ N. Smirnov,⁵² R. Snellings,²⁷ P. Sorensen,³ J. Sowinski,¹⁵ H. M. Spinka,¹ B. Srivastava,³³ A. Stadnik,¹¹ T. D. S. Stanislaus,⁴⁶ D. Staszak,⁶ M. Strikhanov,²⁵ B. Stringfellow,³³ A. A. P. Suaide,³⁷ M. C. Suarez,⁸ N. L. Subba,¹⁸ M. Sumera,¹⁰ X. M. Sun,²¹ Y. Sun,³⁸ Z. Sun,²⁰ B. Surrow,²² T. J. M. Symons,²¹ A. Szanto de Toledo,³⁷ J. Takahashi,⁷ A. H. Tang,³ Z. Tang,³⁸ L. H. Tarini,⁵⁰ T. Tarnowsky,²⁴ D. Thein,⁴³ J. H. Thomas,²¹ J. Tian,⁴⁰ A. R. Timmins,⁵⁰ S. Timoshenko,²⁵ D. Tlusty,¹⁰ M. Tokarev,¹¹ V. N. Tram,²¹ A. L. Trattner,⁴ S. Trentalange,⁶ R. E. Tribble,⁴² O. D. Tsai,⁶ J. Ulery,³³ T. Ullrich,³ D. G. Underwood,¹ G. Van Buren,³ M. van Leeuwen,²⁷ A. M. Vander Molen,²⁴ J. A. Vanfossen, Jr.,¹⁸ R. Varma,¹⁴ G. M. S. Vasconcelos,⁷ I. M. Vasilevski,¹² A. N. Vasiliev,³² F. Videbaek,³ S. E. Vigdor,¹⁵ Y. P. Viyogi,¹³ S. Vokal,¹¹ S. A. Voloshin,⁵⁰ M. Wada,⁴³ M. Walker,²² F. Wang,³³ G. Wang,⁶ J. S. Wang,²⁰ Q. Wang,³³ X. Wang,⁴⁴ X. L. Wang,³⁸ Y. Wang,⁴⁴ G. Webb,¹⁹ J. C. Webb,⁴⁶ G. D. Westfall,²⁴ C. Whitten, Jr.,⁶ H. Wieman,²¹ S. W. Wissink,¹⁵ R. Witt,⁴⁵ Y. Wu,⁵¹ W. Xie,³³ N. Xu,²¹ Q. H. Xu,³⁹ Y. Xu,³⁸ Z. Xu,³ P. Yang,²⁰ P. Yepes,³⁶ K. Yip,³ I.-K. Yoo,³⁴ Q. Yue,⁴⁴ M. Zawisza,⁴⁸ H. Zbroszczyk,⁴⁸ W. Zhan,²⁰ S. Zhang,⁴⁰ W. M. Zhang,¹⁸ X. P. Zhang,²¹ Y. Zhang,²¹ Z. P. Zhang,³⁸ Y. Zhao,³⁸ C. Zhong,⁴⁰ J. Zhou,³⁶ R. Zoulkarneev,¹² Y. Zoulkarneeva,¹² and J. X. Zuo⁴⁰

(STAR Collaboration)

- ¹Argonne National Laboratory, Argonne, Illinois 60439, USA
 - ²University of Birmingham, Birmingham, United Kingdom
 - ³Brookhaven National Laboratory, Upton, New York 11973, USA
 - ⁴University of California, Berkeley, California 94720, USA
 - ⁵University of California, Davis, California 95616, USA
 - ⁶University of California, Los Angeles, California 90095, USA
 - ⁷Universidade Estadual de Campinas, Sao Paulo, Brazil
 - ⁸University of Illinois at Chicago, Chicago, Illinois 60607, USA
 - ⁹Creighton University, Omaha, Nebraska 68178, USA
 - ¹⁰Nuclear Physics Institute AS CR, 250 68 Řež/Prague, Czech Republic
 - ¹¹Laboratory for High Energy (JINR), Dubna, Russia
 - ¹²Particle Physics Laboratory (JINR), Dubna, Russia
 - ¹³Institute of Physics, Bhubaneswar 751005, India
 - ¹⁴Indian Institute of Technology, Mumbai, India
 - ¹⁵Indiana University, Bloomington, Indiana 47408, USA
 - ¹⁶Institut de Recherches Subatomiques, Strasbourg, France
 - ¹⁷University of Jammu, Jammu 180001, India
 - ¹⁸Kent State University, Kent, Ohio 44242, USA
 - ¹⁹University of Kentucky, Lexington, Kentucky, 40506-0055, USA
 - ²⁰Institute of Modern Physics, Lanzhou, China
 - ²¹Lawrence Berkeley National Laboratory, Berkeley, California 94720, USA
 - ²²Massachusetts Institute of Technology, Cambridge, Massachusetts 02139-4307, USA
 - ²³Max-Planck-Institut für Physik, Munich, Germany
 - ²⁴Michigan State University, East Lansing, Michigan 48824, USA
 - ²⁵Moscow Engineering Physics Institute, Moscow Russia
 - ²⁶City College of New York, New York City, New York 10031, USA
 - ²⁷NIKHEF and Utrecht University, Amsterdam, The Netherlands
 - ²⁸Ohio State University, Columbus, Ohio 43210, USA
 - ²⁹Old Dominion University, Norfolk, Virginia, 23529, USA
 - ³⁰Panjab University, Chandigarh 160014, India
 - ³¹Pennsylvania State University, University Park, Pennsylvania 16802, USA
 - ³²Institute of High Energy Physics, Protvino, Russia
 - ³³Purdue University, West Lafayette, Indiana 47907, USA
 - ³⁴Pusan National University, Pusan, Republic of Korea
 - ³⁵University of Rajasthan, Jaipur 302004, India
 - ³⁶Rice University, Houston, Texas 77251, USA
 - ³⁷Universidade de Sao Paulo, Sao Paulo, Brazil
 - ³⁸University of Science & Technology of China, Hefei 230026, China
 - ³⁹Shandong University, Jinan, Shandong 250100, China
 - ⁴⁰Shanghai Institute of Applied Physics, Shanghai 201800, China
 - ⁴¹SUBATECH, Nantes, France
 - ⁴²Texas A&M University, College Station, Texas 77843, USA
 - ⁴³University of Texas, Austin, Texas 78712, USA
 - ⁴⁴Tsinghua University, Beijing 100084, China
 - ⁴⁵United States Naval Academy, Annapolis, Maryland 21402, USA
 - ⁴⁶Valparaiso University, Valparaiso, Indiana 46383, USA
 - ⁴⁷Variable Energy Cyclotron Centre, Kolkata 700064, India
 - ⁴⁸Warsaw University of Technology, Warsaw, Poland
 - ⁴⁹University of Washington, Seattle, Washington 98195, USA
 - ⁵⁰Wayne State University, Detroit, Michigan 48201, USA
 - ⁵¹Institute of Particle Physics, CCNU (HZNU), Wuhan 430079, China
 - ⁵²Yale University, New Haven, Connecticut 06520, USA
 - ⁵³University of Zagreb, Zagreb, HR-10002, Croatia
- (Received 12 January 2009; published 24 August 2009)

We report K/π fluctuations from Au + Au collisions at $\sqrt{s_{NN}} = 19.6, 62.4, 130$, and 200 GeV using the STAR detector at the Relativistic Heavy Ion Collider. K/π fluctuations in central collisions show little dependence on incident energy and are on the same order as those from NA49 at the Super Proton

Synchrotron in central Pb + Pb collisions at $\sqrt{s_{NN}} = 12.3$ and 17.3 GeV. We report results for the collision centrality dependence of K/π fluctuations and results for charge-separated fluctuations. We observe that the K/π fluctuations scale with the charged particle multiplicity density.

DOI: 10.1103/PhysRevLett.103.092301

PACS numbers: 25.75.-q, 24.60.Ky

Strangeness enhancement has been predicted to be one of the important signatures of the formation of the quark-gluon plasma (QGP) [1–5]. Recently, a maximum in the ratio of the yields of K^+ and π^+ , K^+/π^+ , has been observed in central Pb + Pb collisions near $\sqrt{s_{NN}} = 7$ GeV [6]. Dynamical fluctuations in the event-by-event K/π ratio in central Pb + Pb collisions at energies near $\sqrt{s_{NN}} = 7$ GeV are larger than those predicted by the transport model UrQMD using the observable σ_{dyn} [7]. The K/π ratio is defined as the ratio the number of charged kaons in one event divided by the number of charged pions in the same event. The observable σ_{dyn} [8] is defined as

$$\sigma_{\text{dyn}} = \text{sgn}(\sigma_{\text{data}}^2 - \sigma_{\text{mixed}}^2) \sqrt{|\sigma_{\text{data}}^2 - \sigma_{\text{mixed}}^2|} \quad (1)$$

where σ_{data} is the relative width (standard deviation divided by the mean) of the K/π distribution for the data and σ_{mixed} is the relative width of the K/π distribution for mixed events. These observations have generated speculation that a phase transition from hadronic matter to quark-gluon matter may be taking place at incident energies around $\sqrt{s_{NN}} = 7$ GeV [6]. The study of dynamic fluctuations in the event-by-event K/π ratio may produce information concerning QCD phase transitions such as the order of the transitions and the location of the transitions, and may lead to the observation of the critical point of QCD [9,10]. These data for K/π fluctuations may also provide a rigorous test of the statistical hadronization model [11–14].

In this Letter, we report results for dynamic fluctuations of the K/π ratio in central Au + Au collisions at $\sqrt{s_{NN}} = 19.6, 62.4, 130,$ and 200 GeV using the quantity σ_{dyn} [8]. These results are compared with the results of NA49 for dynamical K/π fluctuations in central Pb + Pb collisions [7]. To study the collision centrality dependence of K/π fluctuations, we propose the variable, $\nu_{\text{dyn},K\pi}$, which quantifies the deviation of the fluctuations in the number of pions and kaons from that expected from Poisson statistics. This variable is defined as

$$\nu_{\text{dyn},K\pi} = \frac{\langle K(K-1) \rangle}{\langle K \rangle^2} + \frac{\langle \pi(\pi-1) \rangle}{\langle \pi \rangle^2} - \frac{2\langle K\pi \rangle}{\langle K \rangle \langle \pi \rangle} \quad (2)$$

where K and π are the number of kaons and pions in each event, respectively. The properties of Eq. (2) are discussed at length in Ref. [15]. Negative values of $\nu_{\text{dyn},K\pi}$ imply that the third term in Eq. (2) involving $K-\pi$ correlations dominates, while positive values of $\nu_{\text{dyn},K\pi}$ imply that the first two terms involving the joint correlations $K-K$ and $\pi-\pi$ dominate. We present results for the collision centrality dependence of $\nu_{\text{dyn},K\pi}$ for Au + Au collisions at

62.4 and 200 GeV. To gain insight concerning the origins of these K/π fluctuations [16], we also present the collision centrality dependence of $\nu_{\text{dyn},K\pi}$ for $K^+/\pi^+, K^-/\pi^-, K^+/\pi^-,$ and K^-/π^+ . The observables σ_{dyn} and $\nu_{\text{dyn},K\pi}$ are related as we will discuss below. Both observables represent the dynamic fluctuations of pion and kaon production with the statistical fluctuations removed. These variables are sensitive to acceptance effects that must be considered when comparing with models.

Au + Au collisions were studied at $\sqrt{s_{NN}} = 19.6, 62.4, 130,$ and 200 GeV using the STAR detector at the Relativistic Heavy Ion Collider (RHIC) using a minimum bias trigger. Events accepted took place within ± 15 cm of the center of the STAR detector in the beam direction. Collision centrality was determined using the number of charged tracks within $|\eta| < 0.5$. Nine centrality bins were used corresponding to 0–5% (most central), 5–10%, 10–20%, 20–30%, 30–40%, 40–50%, 50–60%, 60–70%, and 70–80% (most peripheral) of the reaction cross section. To be able to plot our results versus the charged particle multiplicity density, $dN_{\text{ch}}/d\eta$, we associate fully corrected values for $dN_{\text{ch}}/d\eta$ from previously published work with each collision centrality bin [17]. For the 19.6 and 130 GeV data sets, only results from the most central bin are presented. All tracks were required to have originated within 3 cm of the measured event vertex. Only charged particle tracks having more than 15 space points along the trajectory were accepted. The ratio of reconstructed points to possible points along the track was required to be greater than 0.52 to avoid split tracks. In addition to these track quality cuts, we applied event-by-event cuts on the average dip angle of each event versus the event vertex position in the beam direction to suppress events not associated with the measured beam crossing as well as run-to-run cuts on average track parameters to suppress runs with technical problems. Charged pions and charged kaons were identified using the specific energy loss, dE/dx , along the track and the momentum, p , of the track.

Charged pions and kaons were selected with transverse momentum $0.2 < p_t < 0.6$ GeV/c and pseudorapidity $|\eta| < 1.0$. Particle identification was accomplished by selecting particles whose specific energy losses were within 2 standard deviations of the energy loss predictions for a given particle type and momentum. Particle identification for pions (kaons) also included a condition that the specific energy loss should be more than 2 standard deviations away from the loss predicted for a kaon (pion). In addition, electrons were excluded from the analysis for all cases. Particles were excluded as electrons if the specific energy

losses were within 1 standard deviation of the energy loss predictions for electrons. We identify $\sim 90\%$ of the pions in our acceptance. We identify $\sim 50\%$ of the kaons at $p_t = 0.2$ GeV/ c and $\sim 75\%$ of the kaons at $p_t = 0.6$ GeV/ c in our acceptance. We calculate that the fraction of pions resulting from misidentified kaons is negligible while the fraction of kaons resulting from misidentified pions is 6.5%. The electron cut did not affect the pions significantly, but excluded 25% of the kaons for the 200 GeV Au + Au case and 35% of the kaons for the 62.4 GeV Au + Au system. The remaining electron contamination is negligible.

Figure 1 shows the distribution of the event-by-event K/π ratio for central Au + Au collisions (0–5%) at $\sqrt{s_{NN}} = 200$ GeV compared with the same quantity from mixed events. Mixed events were created by taking one track from different events to produce new events with the same multiplicity that have no correlations among particles in those events. Mixed events were produced using ten bins in collision centrality and five bins in event vertex position. The distribution for the data is wider than the distribution for mixed events. Similar results were obtained at the other three incident energies; 19.6, 62.4, and 130 GeV. The same analysis techniques are applied to the mixed events as are applied to the data.

The results for σ_{dyn} from central Au + Au collisions at 19.6, 62.4, 130, and 200 GeV are shown in Fig. 2 along with similar results for central Pb + Pb collisions at $\sqrt{s_{NN}} = 6.3, 7.6, 8.8, 12.3,$ and 17.3 GeV from the NA49 Collaboration [7]. Statistical and systematic errors are shown for both the NA49 results and the STAR results. The systematic errors for σ_{dyn} are discussed in the presentation of the results for $\nu_{\text{dyn}, K\pi}$.

In Fig. 2, we find that the NA49 results show a strong incident energy dependence while the STAR results show little dependence on the incident energy. The STAR results

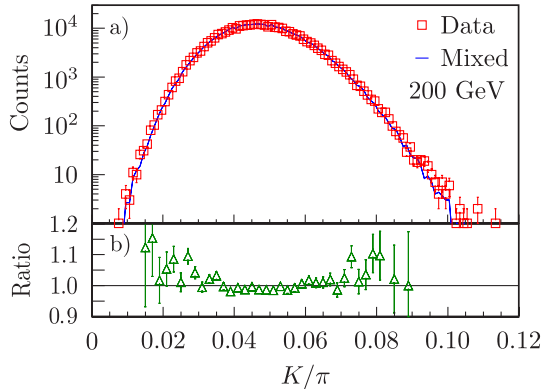


FIG. 1 (color online). (a) The event-by-event K/π ratio for 200 GeV Au + Au central collisions (0–5%) compared with the same quantity calculated from mixed events. (b) The ratio of the distribution from real events to that from mixed events. The errors shown are statistical.

are consistent with the highest energy NA49 result, although the statistical error bar for the 19.6 GeV case is large. In this figure, we compare the statistical hadronization model results of Torrieri [11] to the experimental data. We see that when the light quark phase space occupancy, γ_q , is one, corresponding to equilibrium, the calculations underestimate the experimental results at all energies. When γ_q is varied to reproduce the excitation function of K^+/π^+ yield ratios over the SPS and RHIC energy ranges [11,14], the statistical hadronization model correctly predicts the dynamical fluctuations at the higher energies but underpredicts the NA49 data at the lower energies, supporting the conclusion that the lower energy fluctuation data are anomalous [7]. In these fits, $\gamma_q > 1$ (chemically oversaturated) for $\sqrt{s_{NN}} < 9$ GeV and $\gamma_q < 1$ (chemically undersaturated) for $\sqrt{s_{NN}} > 9$ GeV.

We propose to study K/π fluctuations using a variable that does not involve the K/π ratio directly. We choose to employ the variable $\nu_{\text{dyn}, K\pi}$, which is similar to the observable $\nu_{+-,\text{dyn}}$ [18] used to study net charge fluctuations. $\nu_{\text{dyn}, K\pi}$ does not require mixed events and does not depend on detector efficiencies. Figure 3 shows $\nu_{\text{dyn}, K\pi}$ for 62.4 and 200 GeV Au + Au collisions plotted as a function of $dN_{\text{ch}}/d\eta$. We conservatively estimate the systematic error in $\nu_{\text{dyn}, K\pi}$ due to losses from the electron cut to be 15%. Using HIJING [19], we estimate that the effect of feed down on $\nu_{\text{dyn}, K\pi}$ from weakly decaying particles is 9%. HIJING calculations show that increasing the accepted range in p_t from $0.2 < p_t < 0.6$ GeV/ c to $0.1 < p_t < 2.0$ GeV/ c decreases $\nu_{\text{dyn}, K\pi}$ by less than 5% at both 62.4 and 200 GeV. Thus, the total systematic error in $\nu_{\text{dyn}, K\pi}$ is 18%.

In Fig. 3, we plot the NA49 results using the identity $\sigma_{\text{dyn}}^2 = \nu_{\text{dyn}, K\pi}$. We verified the validity of this identity

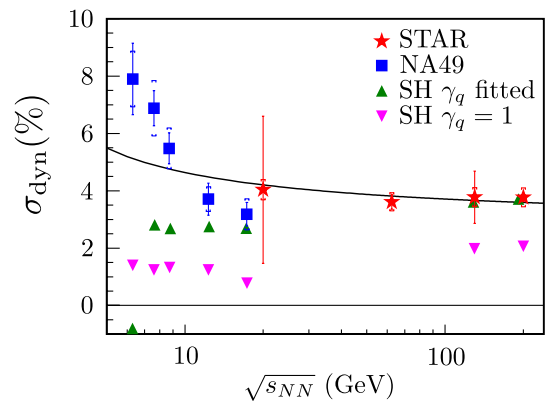


FIG. 2 (color online). Measured K/π fluctuations in terms of σ_{dyn} for central Au + Au collisions (0–5%) at 19.6, 62.4, 130, and 200 GeV compared with the central Pb + Pb collisions (0–3.5%) from NA49 [7] and the statistical hadronization (SH) model of Ref. [11]. The solid line is described in the text. Both statistical (horizontal bar) and systematic (bracket) error bars are shown for the experimental data.

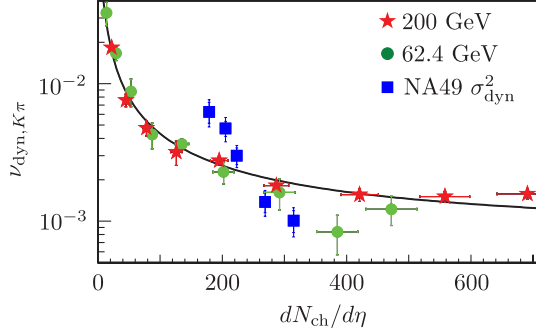


FIG. 3 (color online). Measured K/π fluctuations in terms of $\nu_{\text{dyn},K\pi}$ for 62.4 and 200 GeV Au + Au compared with σ_{dyn}^2 from central Pb + Pb collisions at 6.3, 7.6, 8.8, 12.3, and 17.3 GeV from NA49 [7]. Statistical errors are shown for the STAR data. Statistical and systematic errors are shown for the NA49 results. The solid line corresponds to a fit to the STAR data of the form $c + d/(dN_{\text{ch}}/d\eta)$.

explicitly by calculating both quantities for 62.4 and 200 GeV Au + Au collisions. We find that $\sigma_{\text{dyn}}^2 = \nu_{\text{dyn},K\pi}$ within errors for all centrality bins except the two most peripheral bins at 62.4 GeV. In Fig. 3, we make the correspondence between the incident energy for the NA49 results and $dN_{\text{ch}}/d\eta$ using the systematics in Ref. [20]. The solid line in Fig. 3 represents a fit to the STAR data of the form $c + d/(dN_{\text{ch}}/d\eta)$ where c and d are constants. We choose this functional form because we expect $\nu_{\text{dyn},K\pi}$ to scale with the inverse of the multiplicity. The fit for $\nu_{\text{dyn},K\pi}$ versus $dN_{\text{ch}}/d\eta$ has a χ^2 of 26.6 for 16 degrees of freedom. If we make a similar fit for $\nu_{\text{dyn},K\pi}$ versus N_{part} , we obtain a χ^2 of 50.7 for 16 degrees of freedom. Thus, the fit for $\nu_{\text{dyn},K\pi}$ versus $dN_{\text{ch}}/d\eta$ is significantly better than the fit for $\nu_{\text{dyn},K\pi}$ versus N_{part} . The NA49 results shown in Fig. 3 show a steeper dependence on $dN_{\text{ch}}/d\eta$ than the STAR data and have a χ^2 of 50.8 for 5 degrees of freedom compared to the best fit to the STAR data.

Using the results of the fit for $dN_{\text{ch}}/d\eta$, we can determine the value of $\nu_{\text{dyn},K\pi}$ as a function of $dN_{\text{ch}}/d\eta$. We can then make a correspondence between incident energy and $dN_{\text{ch}}/d\eta$ for central collisions using the systematics in Ref. [20]. Finally, employing the relationship $\sigma_{\text{dyn}}^2 = \nu_{\text{dyn},K\pi}$, we can draw the solid line shown in Fig. 2, which relates the incident energy dependence of σ_{dyn} in central collisions to the collision centrality dependence of $\nu_{\text{dyn},K\pi}$ at higher energies. This line shows a slight increase as the incident energy is lowered, while the NA49 results show a steeper increase as the energy is lowered. Thus, the incident energy dependence of the NA49 results is not simply due to the change in multiplicity as the incident energy is lowered.

In order to gain insight into the origin of these K/π fluctuations, we calculate $\nu_{\text{dyn},K\pi}$ for K^+/π^+ , K^-/π^- , K^+/π^- , and K^-/π^+ . We observe that, within errors,

$\nu_{\text{dyn},K^+\pi^+}$ is equal to $\nu_{\text{dyn},K^-\pi^-}$ and $\nu_{\text{dyn},K^+\pi^-}$ is equal to $\nu_{\text{dyn},K^-\pi^+}$. We report the average of the fluctuations of the ratios K^+/π^+ and K^-/π^- as same sign and the average of the fluctuations of the ratios K^+/π^- and K^-/π^+ as opposite sign in Fig. 4 along with results for K/π as a function of $dN_{\text{ch}}/d\eta$. Because $\nu_{\text{dyn},K\pi}$ approximately scales with the inverse multiplicity, we multiply our results for $\nu_{\text{dyn},K\pi}$ by $dN_{\text{ch}}/d\eta$ to study the collision centrality dependence more effectively.

The scaled $\nu_{\text{dyn},K\pi}$ results for all cases in Fig. 4 increase as the collisions become more central. The scaled results for the summed signs are always positive. The scaled results for the opposite sign are always negative indicating a strong correlation for opposite sign particles. One might expect such negative opposite sign correlations from processes such as the decay $K^*(892) \rightarrow K^+ + \pi^-$. The scaled $\nu_{\text{dyn},K\pi}$ for the same sign are slightly negative in peripheral collisions and slightly positive in central collisions, crossing zero around $dN_{\text{ch}}/d\eta = 400$. The fact that $\nu_{\text{dyn},K\pi}$ for same sign particles is close to zero indicates that the correlations between same sign particles are small.

Also shown in Fig. 4 are HIJING calculations for 62.4 and 200 GeV Au + Au collisions with the acceptance cuts of $|\eta| < 1.0$ and $0.2 < p_t < 0.6$ GeV/c applied, which are the same cuts as applied to the data. In contrast to the experimental results, HIJING predicts no collision centrality dependence or incident energy dependence for $(dN_{\text{ch}}/d\eta)\nu_{\text{dyn},K\pi}$. Therefore, we show the HIJING predictions as horizontal lines. HIJING predicts that the summed sign fluctuations are always positive (dash-dotted line), the same sign fluctuations are always zero (dotted line), and the opposite sign fluctuations are always negative (dashed line). One explanation for the increase in the measured

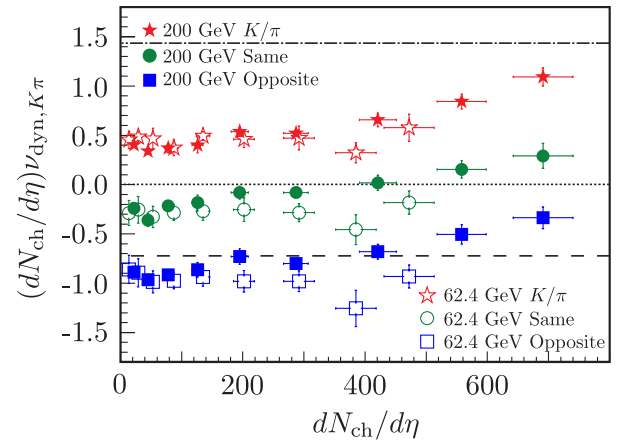


FIG. 4 (color online). The $dN_{\text{ch}}/d\eta$ scaled K/π fluctuations for summed charges (stars), same signs (circles), and opposite signs (squares) as a function of $dN_{\text{ch}}/d\eta$. The errors shown are statistical. The dash-dotted, dotted, and dashed lines represent HIJING calculations for summed charges, same signs, and opposite signs, respectively.

same sign and opposite sign fluctuations scaled with $dN_{\text{ch}}/d\eta$ may be that in peripheral collisions, products of the decay of resonances emerge without further interaction, leading to negative values of $\nu_{\text{dyn},K\pi}$. In central collisions, the daughters of the decay of resonances are rescattered in or out of our acceptance, leading to more positive values of $\nu_{\text{dyn},K\pi}$. For example, the decay of $K_1(1270)^+ \rightarrow K^+ + \rho^0 \rightarrow K^+ + \pi^+ + \pi^-$ would lead to negative same sign fluctuations in peripheral collisions but not in central collisions. Another explanation may be the onset of radial flow in central collisions.

In conclusion, we find that the fluctuations in the K/π ratio for central Au + Au collisions at $\sqrt{s_{NN}} = 19.6, 62.4, 130,$ and 200 GeV are of the same order as the fluctuations observed in central Pb + Pb collisions at $\sqrt{s_{NN}} = 6.3, 7.6, 8.8, 12.3,$ and 17.3 GeV using the variable σ_{dyn} , but the Pb + Pb results show a stronger incident energy dependence. The statistical hadronization model of Ref. [11] cannot reproduce the incident energy dependence of these fluctuations. The collision centrality dependence of K/π fluctuations for Au + Au collisions at $\sqrt{s_{NN}} = 62.4$ and 200 GeV as characterized by the variable $\nu_{\text{dyn},K\pi}$ seems to scale with $dN_{\text{ch}}/d\eta$. Relating the observed centrality dependence of these fluctuations observed in Au + Au collisions at $\sqrt{s_{NN}} = 62.4$ and 200 GeV using $\nu_{\text{dyn},K\pi}$ to the incident energy dependence of fluctuations in central collisions using σ_{dyn} , we find a smooth scaling, decreasing slightly with increasing incident energy. The scaled values fall in the middle of the fluctuations observed by NA49 between $\sqrt{s_{NN}} = 6.3$ and 17.3 GeV. More measurements are required to demonstrate if there is any discontinuity in K/π fluctuations as a function of incident energy. $\nu_{\text{dyn},K\pi}$ results using pions and kaons with the same sign are close to zero while results using $\nu_{\text{dyn},K\pi}$ for opposite sign pions and kaons are negative. The results for $\nu_{\text{dyn},K\pi}$ scaled by $dN_{\text{ch}}/d\eta$ increase as the collisions become more central, unlike the predictions of HIJING that show no centrality dependence. These results may indicate that, due to later stage hadronic rescattering, the decay products of resonances are less likely to survive in central collisions than in peripheral collisions, or may be due to the onset of radial flow combined with our acceptance in p_T .

We thank the RHIC Operations Group and RCF at BNL, and the NERSC Center at LBNL and the resources provided by the Open Science Grid consortium for their support. This work was supported in part by the Offices of NP and HEP within the U.S. DOE Office of Science, the U.S. NSF, the Sloan Foundation, the DFG cluster of excellence “Origin and Structure of the Universe,” CNRS/IN2P3, RA, RPL, and EMN of France, STFC and EPSRC of the United Kingdom, FAPESP of Brazil, the Russian Ministry of Sci. and Tech., the NNSFC, CAS, MoST, and MoE of China, IRP and GA of the Czech Republic, FOM of the Netherlands, DAE, DST, and CSIR of the Government of India, the Polish State Committee for Scientific Research, and the Korea Sci. & Eng. Foundation.

-
- [1] J. Rafelski and B. Müller, Phys. Rev. Lett. **48**, 1066 (1982).
 - [2] S. Soff *et al.*, Phys. Lett. B **471**, 89 (1999).
 - [3] V. Koch, A. Majumder, and J. Randrup, Phys. Rev. C **72**, 064903 (2005).
 - [4] V. Koch, A. Majumder, and J. Randrup, Phys. Rev. Lett. **95**, 182301 (2005).
 - [5] M. I. Gorenstein, M. Gaździcki, and O. S. Zozulya, Phys. Lett. B **585**, 237 (2004).
 - [6] C. Alt *et al.*, Phys. Rev. C **77**, 024903 (2008).
 - [7] C. Alt *et al.*, Phys. Rev. C **79**, 044910 (2009).
 - [8] S. V. Afanasiev *et al.*, Phys. Rev. Lett. **86**, 1965 (2001).
 - [9] M. Stephanov, K. Rajagopal, and E. Shuryak, Phys. Rev. Lett. **81**, 4816 (1998).
 - [10] M. A. Stephanov, Nucl. Phys. A **698**, 523c (2002).
 - [11] G. Torrieri, Int. J. Mod. Phys. E **16**, 1783 (2007).
 - [12] G. Torrieri, arXiv:0901.0221v2.
 - [13] G. Torrieri, J. Phys. G **35**, 044009 (2009).
 - [14] J. Rafelski and J. Letessier, Eur. Phys. J. A **29**, 107 (2006).
 - [15] C. Pruneau, S. Gavin, and S. Voloshin, Phys. Rev. C **66**, 044904 (2002).
 - [16] S. Mrówczyński, Phys. Lett. B **459**, 13 (1999).
 - [17] B. I. Abelev *et al.*, Phys. Rev. C **79**, 034909 (2009).
 - [18] J. Adams *et al.*, Phys. Rev. C **68**, 044905 (2003).
 - [19] X. N. Wang and M. Gyulassy, Phys. Rev. D **44**, 3501 (1991), version 1.38.
 - [20] B. Back *et al.*, Phys. Rev. C **74**, 021902(R) (2006).